

# Optimal quantum cloning of orbital angular momentum photon qubits through Hong–Ou–Mandel coalescence

Eleonora Nagali<sup>1</sup>, Linda Sansoni<sup>1</sup>, Fabio Sciarrino<sup>1,2\*</sup>, Francesco De Martini<sup>1,3</sup>, Lorenzo Marrucci<sup>4,5\*</sup>, Bruno Piccirillo<sup>4,6</sup>, Ebrahim Karimi<sup>4</sup> and Enrico Santamato<sup>4,6</sup>

**The orbital angular momentum (OAM) of light, associated with a helical structure of the wavefunction, has great potential in quantum photonics, as it allows a higher dimensional quantum space to be attached to each photon<sup>1,2</sup>. Hitherto, however, the use of OAM has been hindered by difficulties in its manipulation. Here, by making use of the recently demonstrated spin-OAM information transfer tools<sup>3,4</sup>, we report the first observation of the Hong–Ou–Mandel coalescence<sup>5</sup> of two incoming photons having non-zero OAM into the same outgoing mode of a beamsplitter. The coalescence can be switched on and off by varying the input OAM state of the photons. Such an effect has then been used to carry out the  $1 \rightarrow 2$  universal optimal quantum cloning of OAM-encoded qubits<sup>6–8</sup>, using the symmetrization technique already developed for polarization<sup>9,10</sup>. These results are shown to be scalable to quantum spaces of arbitrary dimensions, even combining different degrees of freedom of the photons.**

The orbital angular momentum (OAM) of photons lies in an infinitely dimensional Hilbert space, so it is a natural choice for implementing single-photon qudits, the units of quantum information in a higher dimensional space. This can be important practically, as it allows the information content per photon to be increased, and this, in turn, may cut down substantially the noise and losses arising from imperfect generation and detection efficiency by reducing the total number of photons needed in a given process. Qudit-based quantum information protocols may also offer better theoretical performances than their qubit equivalents<sup>11,12</sup>, and the combined use of the different degrees of freedom of a photon, such as OAM and spin, enables the implementation of entirely new quantum tasks<sup>13–15</sup>. Finally, an OAM state of light can also be regarded as an elementary form of optical image, so that OAM manipulation is related to quantum image processing<sup>16</sup>.

All these applications are presently hindered by the technical difficulties associated with OAM manipulation. Despite important successes, particularly in the generation and application of OAM-entangled<sup>17–19</sup> and OAM/polarization hyperentangled photons<sup>13,14</sup>, a classic two-photon quantum interference process such as the Hong–Ou–Mandel (HOM) effect<sup>5</sup> has not been demonstrated yet for photons carrying non-zero OAM. In the case of the polarization degree of freedom, this phenomenon has played a crucial role in many recent developments of quantum information, as well as in fundamental studies of quantum non-locality. For example, it has been exploited for the implementation of quantum teleportation<sup>20,21</sup>, the construction of quantum logic

gates for quantum information processing<sup>22</sup>, the optimal cloning of a quantum state<sup>9,10</sup>, and various other applications<sup>23</sup>. Hitherto, none of these applications has been demonstrated with OAM quantum states.

Quantum cloning—making copies of unknown input quantum states—represents a particularly important and interesting example of an application. The impossibility of making perfect copies, dictated by the ‘no-cloning’ theorem<sup>24</sup>, is a fundamental piece of modern quantum theory and guarantees the security of quantum cryptography<sup>25</sup>. Even though perfect cloning cannot be realized, it is still possible to single out a complete positive map that yields an optimal quantum cloning<sup>8</sup> working for any input state, that is, universal. With this map, an arbitrary, unknown quantum state can be experimentally copied, but only with a cloning fidelity  $F$  (the overlap between the copy and the original quantum state) less than unity. Implementing quantum cloning is useful whenever there is the need to distribute quantum information among several parties. The concept also finds application in the security assessment of quantum cryptography, the realization of minimal disturbance measurements, in enhancing the transmission fidelity over a lossy quantum channel, and in separating classical and quantum information<sup>8,26</sup>. Optimal quantum cloning machines, although working probabilistically, have been demonstrated experimentally for polarization-encoded photon qubits by stimulated emission<sup>6,7</sup> and by the symmetrization technique<sup>9,10,27</sup>. In the latter method, the bosonic nature of photons (that is, the symmetry of their overall wavefunction) is used within a two-photon HOM coalescence effect. In this process, two photons impinging simultaneously on a beamsplitter from two different input modes have an enhanced probability of emerging along the same output mode (that is, coalescing), as long as they are indistinguishable. If the two photons are made distinguishable by their internal quantum state, for example encoded in the polarization  $\pi$  or in other degrees of freedom, the coalescence effect vanishes. Now, if one of the two photons involved in the process is in a given input state to be cloned and the other in a random one, the HOM effect will enhance the probability that the two photons emerge from the beamsplitter with the same quantum state, that is, with successful cloning, when they emerge together along the same output mode of the beamsplitter. For qubit states, the ideal success probability of this scheme is  $p = 3/4$  (when using both beamsplitter exit ports), and the cloning fidelity for successful events is  $F = 5/6$ , corresponding to the optimal value<sup>27</sup>. The probabilistic feature of this implementation does not spoil its optimality, as it has been

<sup>1</sup>Dipartimento di Fisica, Sapienza Università di Roma, Roma 00185, Italy, <sup>2</sup>Istituto Nazionale di Ottica Applicata, Firenze 50125, Italy, <sup>3</sup>Accademia Nazionale dei Lincei, via della Lungara 10, Roma 00165, Italy, <sup>4</sup>Dipartimento di Scienze Fisiche, Università di Napoli ‘Federico II’, Compl. Univ. di Monte S. Angelo, 80126 Napoli, Italy, <sup>5</sup>CNR-INFM Coherentia, Compl. Univ. di Monte S. Angelo, 80126 Napoli, Italy, <sup>6</sup>Consorzio Nazionale Interuniversitario per le Scienze Fisiche della Materia, Napoli. \*e-mail: fabio.sciarrino@uniroma1.it; lorenzo.marrucci@na.infn.it

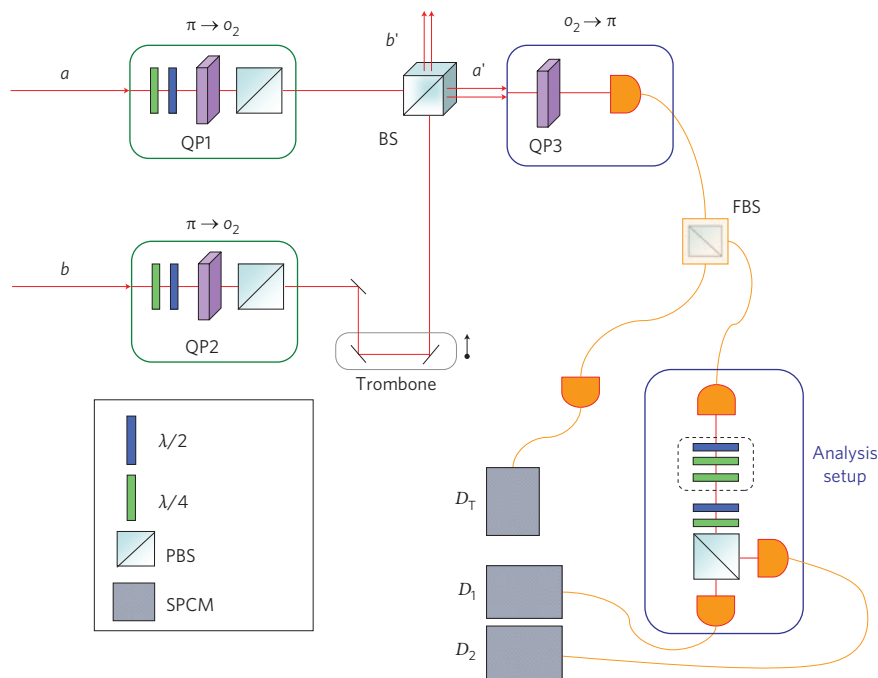


**Figure 1 | Experimental setup for demonstrating the Hong-Ou-Mandel (HOM) effect and for implementing OAM quantum cloning.** In the experiments, two photons generated by parametric fluorescence and having the same wavefunction (see Methods) are injected into the two input modes  $a$  and  $b$ . To set the input OAM state  $|\varphi\rangle_{o_2}$  of a photon, the same state is first encoded in the polarization space  $\pi$ , that is, the state  $|\varphi\rangle_{\pi}$  is prepared by using a combination of a quarter-wave plate ( $\lambda/4$ ) and a half-wave plate ( $\lambda/2$ ), and then the  $\pi \rightarrow o_2$  quantum transfer device<sup>4</sup> is used. In particular, a transferrer composed of a q-plate (QP1 in mode  $a$  and QP2 in  $b$ ) and a polarizer (PBS) filtering the horizontal ( $H$ ) polarization achieves the transformation  $|\varphi\rangle_{\pi}|0\rangle_o \rightarrow |H\rangle_{\pi}|\varphi\rangle_{o_2}$ , where  $|0\rangle_o$  denotes the zero-OAM state. By this method, the input OAM state of each of the input photons was set independently. The photons in modes  $a$  and  $b$  then, after a time synchronization controlled by the trombone device, interfere in the balanced beamsplitter (BS), giving rise to the HOM effect and/or to the cloning process in the beamsplitter output mode  $a'$ . To analyse the OAM quantum state of the outgoing photons, a  $o_2 \rightarrow \pi$  transferrer<sup>4</sup> is first used. This device, combining a q-plate and a coupler into a single-mode fibre, achieves the inverse transformation  $|H\rangle_{\pi}|\varphi\rangle_{o_2} \rightarrow |\varphi\rangle_{\pi}|0\rangle_o$ , thus transferring the quantum information contained in the two photons back into the polarization degree of freedom, where it can be easily read out. The two photons coupled in the single mode fibre are then separated by a fibre integrated beamsplitter (FBS) and detected in coincidence, after analysing the polarization of one of them by a standard analysis setup. The signal is given by the coincidences between single-photon counting module (SPCM) detectors  $D_T$  and either  $D_1$  or  $D_2$ , thus corresponding to a post-selection of the sole cases in which both photons emerge from the beamsplitter in mode  $a'$  and are then split by the FBS.

proved that the optimal cloning fidelity is the same for any probabilistic procedure<sup>28</sup>.

In this paper, we report the first observation of two-photon HOM coalescence interference of photons carrying non-zero OAM. Furthermore, we use this result to demonstrate for the first time the  $1 \rightarrow 2$  universal optimal quantum cloning (UOQC) of the OAM quantum state of a single photon. More specifically, we show that we can optimally clone any qubit state  $|\varphi\rangle_{o_2}$  encoded in the photon OAM bidimensional subspace  $o_2$ , spanned by the eigenstates  $\{|+2\rangle, |-2\rangle\}$  respectively corresponding to an OAM of  $+2$  and  $-2$ , in units of  $\hbar$ . A key technical development that made these results possible is given by the polarization-OAM bidirectional quantum transfer devices that we have recently demonstrated<sup>4</sup>, the working principle of which is based on the spin-to-orbital optical angular momentum conversion process taking place in the so-called q-plates<sup>3</sup>.

As we work in a bidimensional subspace of the OAM, it is possible to construct a ‘Poincaré’ (or Bloch) sphere to represent the state of an OAM qubit that is fully analogous to the one usually constructed for a polarization qubit<sup>29</sup>. With  $\{|+2\rangle, |-2\rangle\}$  being the basis in the OAM subspace  $o_2$ , which can be considered the OAM equivalent of the circular polarization states, we may introduce the following superposition states  $|h\rangle = (|+2\rangle + |-2\rangle)/\sqrt{2}$ ,  $|v\rangle = (|+2\rangle - |-2\rangle)/i\sqrt{2}$ ,  $|a\rangle = (|h\rangle + |v\rangle)/\sqrt{2}$ , and  $|d\rangle = (|h\rangle - |v\rangle)/\sqrt{2}$ , which are the OAM equivalent of horizontal/vertical and anti-diagonal/diagonal linear polarizations. The OAM eigenstates  $|+2\rangle, |-2\rangle$  have the azimuthal transverse pattern of the

Laguerre–Gauss (LG) modes, whereas states  $|h\rangle, |v\rangle$  (as well as  $|a\rangle, |d\rangle$ ) have the azimuthal structure of the Hermite–Gauss (HG) modes.

As a first experimental step, we carried out a HOM coalescence enhancement measurement. To this purpose, we prepared the two input photons in a given input OAM degree of freedom (see Fig. 1 for details). The time delay controller device and the input polarizers guarantee perfect temporal and polarization matching of the two photons to make them indistinguishable, except possibly in the OAM state. We expect to observe constructive interference between the two photons only if the OAM contribution to the bosonic wavefunction is also symmetric in the output, that is, if the two outgoing photons have the same OAM. Note that the beamsplitter is not an OAM-preserving optical device, as the reflection on the beamsplitter inverts the sign of the OAM. Therefore, the maximal two-photon coalescence is expected to be observed when the input photons carry exactly opposite OAM. Moreover, coalescence is expected when they have the same HG-like state, for example,  $|h\rangle$  or  $|v\rangle$ . Figure 2 shows the results of our experiments. As expected, we find a peak in the coincidence counts when the photon arrivals on the beamsplitter are synchronized and the OAM output states are identical. When the OAM output states are orthogonal the coalescence effect is fully cancelled. The mean coincidence-counts enhancement observed in the two HOM experiments is  $R = (1.97 \pm 0.05)$ , in agreement with the theoretical value of 2.

We now move on to the OAM cloning experiment. Let us first briefly describe the theory of the UOQC process in the OAM

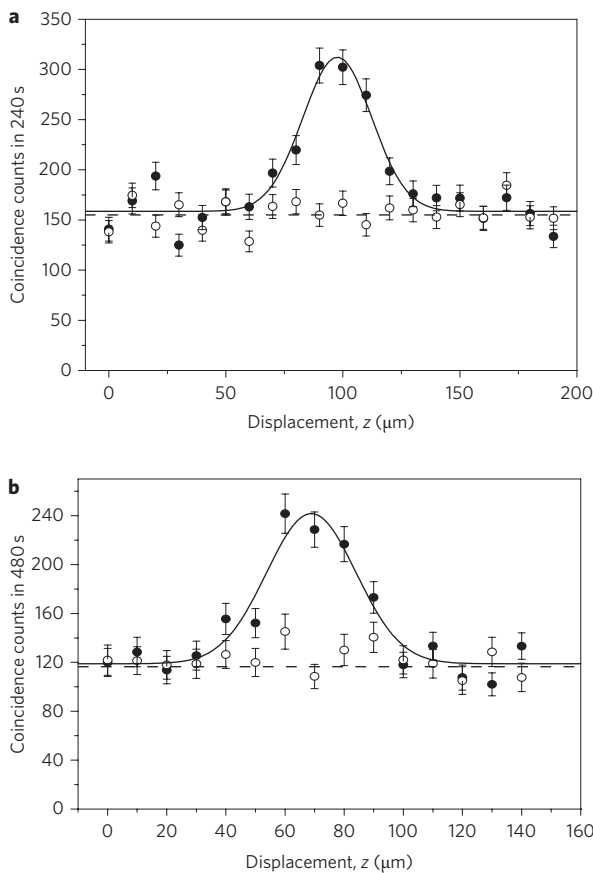


**Figure 2 | Experimental Hong-Ou-Mandel (HOM) effect with OAM.** **a**, Input photons having opposite-OAM eigenstates  $|+2\rangle$  and  $|-2\rangle$  (filled circles) and equal-OAM eigenstates  $|+2\rangle$  (open circles). The first case leads to coalescence enhancement when the photons are synchronized by the trombone displacement, and the second case shows no enhancement. The solid curve is a best fit based on theoretical prediction. **b**, Input photons having the same HG-like OAM-superposition state  $|h\rangle$  (filled circles) and orthogonal HG-like states  $|h\rangle$  and  $|v\rangle$  (open circles). The error bars assume a Poisson distribution and are set at one standard deviation.

**Table 1 | Experimental fidelities for the cloning process.**

State	Fidelity
$ h\rangle_{o_2}$	$(0.806 \pm 0.023)$
$ v\rangle_{o_2}$	$(0.835 \pm 0.015)$
$ -2\rangle_o$	$(0.792 \pm 0.024)$
$ +2\rangle_o$	$(0.769 \pm 0.022)$
$ a\rangle_{o_2}$	$(0.773 \pm 0.020)$
$ d\rangle_{o_2}$	$(0.844 \pm 0.019)$

The experimental values of the fidelity are reported for six specific OAM states.

subspace  $o_2$ . The OAM qubit to be cloned,  $|\varphi\rangle_{o_2} = \alpha|+2\rangle + \beta|-2\rangle$ , is attributed to the photon in input mode  $a$ . The photon in input mode  $b$  is prepared in the mixed state described by density matrix  $\rho_{o_2}^b = (|+2\rangle\langle+2| + |-2\rangle\langle-2|)/2$ . The two photons are then made to interfere in the beamsplitter. By selecting the cases in which the two photons emerge from the beamsplitter in the same output mode  $a'$ , the overall two-photon state is then subject to the following projection operator:  $P^{a'} = (|\Psi^+\rangle^{a'}\langle\Phi^+|^{ab} + |\Phi^+\rangle^{a'}\langle\Psi^+|^{ab} + |\Phi^-\rangle^{a'}\langle\Psi^-|^{ab} + |\Psi^-\rangle^{a'}\langle\Phi^-|^{ab})$  with  $|\Phi^\pm\rangle = 2^{-1/2}(|+2\rangle + |\pm 2\rangle)$  and  $|\Psi^\pm\rangle = 2^{-1/2}(|+2\rangle - |\pm 2\rangle)$ . Note that this projection operator takes into account the fact that the photon OAM undergoes a sign inversion on reflection in the beamsplitter. The two photons emerging in mode  $a'$  are

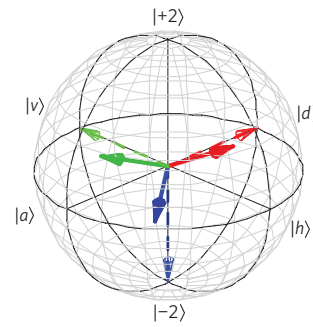


**Figure 3 | Experimental shrunk Bloch sphere of the OAM cloned qubits in the subspace  $o_2$ .** The dashed arrows refer to the theoretical input qubits, and the solid arrows indicate the experimental output qubits.

then separated by means of a second beamsplitter and each of them will be cast in the same mixed qubit state

$$\rho_{o_2}^{a'} = \frac{5}{6}|\varphi\rangle_{o_2}\langle\varphi| + \frac{1}{6}|\varphi^\perp\rangle_{o_2}\langle\varphi^\perp| \quad (1)$$

which represents the optimal output of the  $1 \rightarrow 2$  cloning process of the state  $|\varphi\rangle_{o_2}$ , with fidelity  $F = {}_{o_2}\langle\varphi|\rho_{o_2}^{a'}|\varphi\rangle_{o_2} = \frac{5}{6}$ .

Experimentally, the mixed state  $\rho_{o_2}^b$  has been prepared by randomly rotating, during each experimental run, a half-wave plate inserted before the q-plate QP2 (Fig. 1). In Table 1, we report the experimental fidelities of the cloning process for six different input states  $|\varphi\rangle_{o_2}$  to verify the universality of the cloning process (see Methods for further details). The measured values are in good agreement with the theoretical prediction  $F = 5/6$  (see Methods). For the sake of completeness, we have also measured the four Stokes parameters<sup>29</sup> of some cloned states. The results are reported in Fig. 3. Experimentally, the mean length of the vectors on the Bloch sphere representing the cloned states is found to be  $S_{\text{exp}} = 0.68 \pm 0.02$ , to be compared with the theoretical value  $S_{\text{th}} = 2F - 1 = 2/3$ . The value of  $S_{\text{exp}}$  has been estimated to be  $S_{\text{exp}} = \sqrt{S_1^2 + S_2^2 + S_3^2}$ , where  $S_i$  refers to the  $i$ th measured Stokes component on the Bloch sphere. Hence, the optimal cloning process corresponds to a shrinking of the whole Bloch sphere in the subspace  $o_2$ . The unitary vector length, related to the visibility of the input qubit, is shortened to two-thirds in the output.

Finally, as shown in the Methods, note that the symmetrization technique that implements the quantum cloning is optimal not only for qubit states, but also for arbitrary dimension  $d$  of the internal spaces of the quantum systems that are cloned (qudits): photons with internal states defined in arbitrarily large subspaces of OAM, or even spanning different internal degrees of freedom at the same time (for example, polarization, time, arbitrary transverse modes), can also be cloned optimally by the same method. The fidelity will be given by  $F = (1/2) + (1/(d+1))$  (ref. 30), while the success probability decreases only weakly with increasing  $d$ , saturating at  $p = 1/2$  in the  $d \rightarrow \infty$  limit.

In conclusion, in this paper we have experimentally carried out the first observation of a two-photon HOM coalescence of photons carrying non-zero OAM and the universal optimal quantum cloning of OAM qubits. These results open the way to the use of OAM in many other quantum information protocols based on two-photon interference effects, such as the generation of complex entangled states (for example, cluster states), purification processes, and the implementation of logic gates.

**Methods**

**Experimental setup.** The input photon pairs were generated through spontaneous parametric fluorescence in a  $\beta$ -barium borate crystal, pumped by the second harmonic of a Ti:sapphire mode-locked laser beam. The generated photons had

horizontal ( $H$ ) and vertical ( $V$ ) linear polarizations, wavelength  $\lambda = 795$  nm, and spectral bandwidth  $\Delta\lambda = 6$  nm, as determined by an interference filter. The detected coincidence rate of the source was  $C_{\text{source}} = 5$  kHz. The photons were delivered to the setup by means of a single-mode fibre, thus defining their transverse spatial mode to a  $\text{TEM}_{00}$ . The photons were then split by a polarizing beamsplitter and injected in the two input modes  $a$  and  $b$  of the apparatus shown in Fig. 1. The quantum transmitters  $\pi \rightarrow o_2$  inserted on modes  $a$  and  $b$  were based on q-plates having a topological charge  $q = 1$ , giving rise to the OAM conversion  $m \rightarrow m \pm 2$  (in units of  $\hbar$ ) in the light beam crossing it, where the  $\pm$  sign is fixed by the input light circular-polarization handedness<sup>3,4</sup>. The conversion efficiency of the q-plates was  $0.80 \pm 0.05$  at 795 nm, due to the reflection on the two faces, imperfect tuning of the q-plate and birefringence pattern imperfections. The overall transducer fidelity within the output OAM subspace was estimated at  $F_{\text{prep}} = (0.96 \pm 0.01)$ , mainly due to the imperfect mode quality of the q-plates, leading to a non-perfect  $\pi \rightarrow o_2$  conversion. The polarization and temporal matching on the beamsplitter between photons on mode  $a$  and  $b$  was achieved within an estimated error fixed by the polarization setting accuracy ( $0.5^\circ$ ) and the positioning sensitivity of the trombone device ( $1 \mu\text{m}$ ).

**Cloning fidelity and success rate estimation.** We set the polarization analysis system to have detectors  $D_1$  and  $D_2$  (Fig. 1) measuring photons respectively in the cloned state  $|\varphi\rangle_{\text{cl}}$  and the orthogonal state  $|\varphi^\perp\rangle_{\text{cl}}$ . The coincidences of either one of these detectors with  $D_T$  ensure also the coalescence of the two photons in the same mode. Let  $C_1, C_2$  denote the coincidence counts of  $D_T$  and  $D_1, D_2$ , respectively. The cloning success rate is then proportional to  $C_{\text{tot}} = C_1 + C_2$ , and the average experimental cloning fidelity is given by  $F_{\text{exp}} = C_1/C_{\text{tot}}$ .

The experimental cloning fidelity is to be compared with the prediction that takes into account the imperfect preparation fidelity  $F_{\text{prep}}$  of the OAM photon state to be cloned (the fidelity of the mixed state is higher than 0.99, due to compensations in the randomization procedure), given by  $F_{\text{th}} = (F_{\text{prep}}R + 1/2)/(R + 1)$ , where  $R$  is the experimental HOM enhancement. The mean value of the experimental cloning fidelity for all our tests reported in Table 1, given by  $\bar{F}_{\text{exp}} = 0.803 \pm 0.008$ , is indeed consistent with the predicted value  $F_{\text{th}} = 0.805 \pm 0.007$ .

The experimental coincidence rate  $C_{\text{tot}}$  can be compared with the predicted one, as determined from  $C_{\text{source}}$  after taking into account three main loss factors: state preparation probability  $p_{\text{prep}}$ , successful cloning probability  $p_{\text{clon}}$  and detection probability  $p_{\text{det}}$ .  $p_{\text{prep}}$  depends on the conversion efficiency of the q-plate and on the probabilistic efficiency of the quantum transducer  $\pi \rightarrow o_2$  (0.5), thus leading to  $p_{\text{prep}} = 0.40 \pm 0.03$ . For ideal input photon states, the experimental success probability of the cloning process on a single beamsplitter output mode is expected to be essentially equal to the theoretical one  $p_{\text{clon}} = 3/8$ . The probability  $p_{\text{det}}$  depends on the q-plate and transducer efficiencies ( $0.8 \times 0.5$ ) plus the fibre coupling efficiency ( $0.15 - 0.25$ ). Hence we have  $p_{\text{det}} = 0.06 - 0.10$ . Therefore, the expected event rate is  $C_{\text{source}} \times p_{\text{prep}} \times p_{\text{clon}} \times p_{\text{det}} \times 1/2 = 0.5 - 1.5$  Hz, where the final factor  $1/2$  takes into account the probability that the two photons are split into different output modes of the analysis FBS. Typically, we had around 400 counts in 600 s, consistent with expectations.

In the present experiment, for practical reasons, we adopted a post-selection technique to identify when two photons emerge from the same output mode. In principle, post-selection could be replaced by quantum non-demolition measurements.

**Generalization of the cloning process to dimension  $d$ .** Let us assume that a photon in the unknown input  $d$ -dimensional state  $|\varphi\rangle$  to be cloned is injected in one arm of a balanced beamsplitter, while the 'ancilla' photon in the other arm is taken to be in a fully mixed state  $\rho = (I_d/d) = (1/d) \sum_n |n\rangle\langle n|$ , where  $|n\rangle$  with  $n = 1, \dots, d$  is an orthonormal basis. Without loss of generality, we may choose a basis for which  $|1\rangle \equiv |\varphi\rangle$ . Depending on the state of the ancilla, we must distinguish two cases in the input: (i) the two-photon state is  $|1\rangle|1\rangle$ , with probability  $1/d$ , or (ii) it is  $|1\rangle|k\rangle$  and  $k \neq 1$ , with probability  $(d-1)/d$ . After interaction in the beamsplitter, we consider only the case of two photons emerging in the same beamsplitter output mode (case of successful cloning). Then, quantum interference leads to a doubled probability for case (i) than for case (ii), so that the output probabilities are respectively rescaled to  $2/(d+1)$  for case (i) and  $(d-1)/(d+1)$  for case (ii). The cloning fidelity is 1 for case (i) and  $1/2$  for case (ii), so that an overall fidelity of  $F = (2/(d+1)) \times 1 + (d-1)/(d+1) \times 1/2 = 1/2 + (1/(d+1))$  is obtained, corresponding to the optimal one, as shown in ref. 30. The success rate of the cloning is  $p = (d+1)/2d$ .

Received 14 May 2009; accepted 19 October 2009;  
published online 22 November 2009

## References

- Molina-Terriza, G., Torres, J. P. & Torner, L. Twisted photons. *Nature Phys.* **3**, 305–310 (2007).
- Franke-Arnold, S., Allen, L. & Padgett, M. Advances in optical angular momentum. *Laser Photon.* **2**, 299–313 (2008).

- Marrucci, L., Manzo, C. & Paparo, D. Optical spin-to-orbital angular momentum conversion in inhomogeneous anisotropic media. *Phys. Rev. Lett.* **96**, 163905 (2006).
- Nagali, E. *et al.* Quantum information transfer from spin to orbital angular momentum of photons. *Phys. Rev. Lett.* **103**, 013601 (2009).
- Hong, C. K., Ou, Z. Y. & Mandel, L. Measurement of subpicosecond time intervals between two photons by interference. *Phys. Rev. Lett.* **59**, 2044 (1987).
- Lamas-Linares, A., Simon, C., Howell, J. C. & Bouwmeester, D. Experimental quantum cloning of single photons. *Science* **296**, 712–714 (2002).
- De Martini, F., Buzek, V., Sciarrino, F. & Sias, C. Experimental realization of the quantum universal NOT gate. *Nature* **419**, 815–818 (2002).
- Scarani, V., Iblisdir, S. & Gisin, N. Quantum cloning. *Rev. Mod. Phys.* **77**, 1225–1256 (2005).
- Ricci, M., Sciarrino, F., Sias, C. & De Martini, F. Teleportation scheme implementing the Universal Optimal Quantum Cloning Machine and the Universal NOT gate. *Phys. Rev. Lett.* **92**, 047901 (2004).
- Irvine, W. T. M., Lamas-Linares, A., de Dood, M. J. A. & Bouwmeester, D. Optimal quantum cloning on a beamsplitter. *Phys. Rev. Lett.* **92**, 047902 (2004).
- Cerf, N. J., Bourennane, M., Karlsson, A. & Gisin, N. Security of quantum key distribution using  $d$ -level systems. *Phys. Rev. Lett.* **88**, 127902 (2002).
- Barbieri, M., De Martini, F., Mataloni, P., Vallone, G. & Cabello, A. Enhancing the violation of the Einstein-Podolsky-Rosen local realism by quantum hyperentanglement. *Phys. Rev. Lett.* **96**, 163905 (2006).
- Barreiro, J. T., Langford, N. K., Peters, N. A. & Kwiat, P. G. Generation of hyperentangled photons pairs. *Phys. Rev. Lett.* **95**, 260501 (2005).
- Barreiro, J. T., Wei, T. C. & Kwiat, P. G. Beating the channel capacity limit for linear photonic superdense coding. *Nature Phys.* **4**, 282–286 (2008).
- Aolita, L. & Walborn, S. P. Quantum communication without alignment using multiple-qubit single-photon states. *Phys. Rev. Lett.* **98**, 100501 (2007).
- Gatti, A., Brambilla, E., Lugiato, L. A. & Kolobov, M. I. Quantum entangled images. *Phys. Rev. Lett.* **83**, 1763 (1999).
- Mair, A., Vaziri, A., Weihs, G. & Zeilinger, A. Entanglement of the orbital angular momentum states of photons. *Nature* **412**, 313–316 (2001).
- Vaziri, A., Pan, J. W., Jennewein, T., Weihs, G. & Zeilinger, A. Concentration of higher dimensional entanglement: qutrits of photon orbital angular momentum. *Phys. Rev. Lett.* **91**, 227902 (2003).
- Langford, N. K. *et al.* Measuring entangled qutrits and their use for quantum bit commitment. *Phys. Rev. Lett.* **93**, 053601 (2004).
- Bouwmeester, D. *et al.* Experimental quantum teleportation. *Nature* **390**, 575–579 (1999).
- Boschi, D., Branca, S., De Martini, F., Hardy, L. & Popescu, S. Experimental realization of teleporting an unknown pure quantum state via dual classical and Einstein-Podolsky-Rosen channels. *Phys. Rev. Lett.* **80**, 1121 (1998).
- Kok, P. *et al.* Linear optical quantum computing with photonic qubits. *Rev. Mod. Phys.* **79**, 135–174 (2007).
- Specht, H. P. *et al.* Phase shaping of single-photon wave packets. *Nature Photon.* **3**, 469–472 (2009).
- Wooters, W. K. & Zurek, W. H. A single quantum cannot be cloned. *Nature* **299**, 802–803 (1982).
- Gisin, N., Ribordy, G., Tittel, W. & Zbinden, H. Quantum cryptography. *Rev. Mod. Phys.* **74**, 145–195 (2002).
- Ricci, M. *et al.* Separating the classical and quantum information via quantum cloning. *Phys. Rev. Lett.* **95**, 090504 (2005).
- Sciarrino, F., Sias, C., Ricci, M. & De Martini, F. Realization of universal optimal quantum machines by projective operators and stochastic maps. *Phys. Rev. A* **70**, 052305 (2004).
- Fiurasek, J. Optimal probabilistic cloning and purification of quantum states. *Phys. Rev. A* **70**, 032308 (2004).
- Padgett, M. J. & Courtial, J. Poincaré-sphere equivalent for light beams containing orbital angular momentum. *Opt. Lett.* **24**, 430–432 (1999).
- Navez, P. & Cerf, N. J. Cloning a real  $d$ -dimensional quantum state on the edge of the no-signaling condition. *Phys. Rev. A*, **68**, 032313 (2003).

## Author contributions

E.N., L.S., F.S., F.D.M., L.M. and E.S. conceived and designed the experiments. E.N., L.S. and F.S. performed the experiments. E.N., L.S. and F.S. analysed the data. L.M., B.P., E.K. and E.S. contributed materials. All authors contributed to the writing of the paper.

## Additional information

Reprints and permission information is available online at <http://npg.nature.com/reprintsandpermissions/>. Correspondence and requests for materials should be addressed to F.S. and L.M.